HAL open science

About the Maximum Principle Violations of the Mixed-Hybrid Finite Element Method applied to Diffusion Equations

Hussein Hoteit, Robert Mosé, Bernard Philippe, Philippe Ackerer, Jocelyne Erhel

To cite this version:

Hussein Hoteit, Robert Mosé, Bernard Philippe, Philippe Ackerer, Jocelyne Erhel. About the Maximum Principle Violations of the Mixed-Hybrid Finite Element Method applied to Diffusion Equations. [Research Report] RR-4227, INRIA. 2001. inria-00072392

HAL Id: inria-00072392

https://inria.hal.science/inria-00072392v1

Submitted on 24 May 2006

HAL is a multi-disciplinary open access archive for the deposit and dissemination of scientific research documents, whether they are published or not. The documents may come from teaching and research institutions in France or abroad, or from public or private research centers.

L'archive ouverte pluridisciplinaire **HAL**, est destinée au dépôt et à la diffusion de documents scientifiques de niveau recherche, publiés ou non, émanant des établissements d'enseignement et de recherche français ou étrangers, des laboratoires publics ou privés.

INSTITUT NATIONAL DE RECHERCHE EN INFORMATIQUE ET EN AUTOMATIQUE

About the Maximum Principle Violations of the Mixed-Hybrid Finite Element Method applied to Diffusion Equations

Hussein Hoteit — Robert Mosé — Bernard Philippe —

Philippe Ackerer — Jocelyne Erhel

N° 4227

Juillet 2001

THÈME 4

Rapport de recherche

ISSN 0249-6399 ISRN INRIA/RR--4227--FR+ENG

About the Maximum Principle Violations of the Mixed-Hybrid Finite Element Method applied to Diffusion Equations

Hussein Hoteit , Robert Mosé *, Bernard Philippe ,
Philippe Ackerer *, Jocelyne Erhel

Thème 4 — Simulation et optimisation
de systèmes complexes
Projet Aladin

Rapport de recherche n° 4227 — Juillet 2001 — 26 pages

Abstract: The affluent literature of finite element methods applied to linear parabolic problems, generally, produces numerical procedures with satisfactory properties from a numerical approximation point of view. However, some initial, boundary conditions or abrupt sink/source terms may cause large gradients at some points and consequently jumps in the solution that usually needs a certain period of time to become more and more smooth. This intuitive fact of the diffusion process necessitates, when applying numerical methods, varying the mesh size (in time and space) according to the smoothness of the solution. In this work, the numerical behavior of the time-dependent solutions for such problems during small time duration obtained by using the Mixed-Hybrid Finite Element Method (MHFEM) is investigated. Numerical comparisons with the standard Galerkin Finite Element (FE) as well as the Finite Difference (FD) methods are checked up on. Due to the fact that the mixed methods violate the discrete maximum principle, some numerical experiments showed that the MHFEM leads sometimes to non-physical peaks in the solution. A diffusivity criterion relating the mesh steps for an artificial initial-boundary value problem will be presented. One of the propositions given to avoid any non-physical oscillations is to use the mass-lumping techniques.

* Institut de Mécanique des Fluides et des solides, Univ. Louis Pasteur de Strasbourg, CNRS/MUR 7507, 2 rue Boussingault, 67000 Strasbourg.

Unité de recherche INRIA Rennes
IRISA, Campus universitaire de Beaulieu, 35042 Rennes Cedex (France)
Téléphone : +33 2 99 84 71 00 —T élécopie : +33 2 99 84 71 71

Key-words: parabolic problem, mixed-hybrid finite method, discrete maximum principle, refinement, mass-lumping.

A propos de la violation du Principe du Maximum par la Méthode des EFMH appliquée aux Equations de Diffusion.

Résumé : L'abondante littérature sur les méthodes de type éléments finis appliquées aux problèmes paraboliques linéaires conclut généralement sur les propriétés satisfaisantes du point de vue de l'approximation numérique. Cependant, certains problèmes aux conditions initiales, aux limites ou aux termes puits/sources raides peuvent entraîner l'apparition de gradients localement très forts, causant ainsi aux temps courts des sauts dans la solution, solution qui devient de plus en plus lisse à mesure que la période de temps augmente. Ce fait rend nécessaire, lors de l'utilisation des méthodes numériques, l'adaptation des pas de temps et d'espace selon la raideur de la solution. Dans ce travail, nous étudions le comportement de la méthode des Eléments Finis Mixtes Hybrides (EFMH) dans le cadre de problèmes diffusifs transitoires plus ou moins raides dans la condition initiale. Des comparaisons numériques avec les méthodes de type Elément Finis standards (EF) et Différences Finies (DF) sont effectuées. Les méthodes mixtes ne respectant pas le principe de maximum discret, quelques expériences numériques montrent que la méthodes des EFMH mène parfois à des pics non-physiques dans la solution. Un critère reliant les pas de temps et d'espace particulier est présenté. Pour remédier à la présence d'oscillations non physiques de la solution obtenue par la méthode des EFMH, une des propositions est d'utiliser la technique de condensation de masse.

Mots-clés : problèmes paraboliques, écoulement en milieu poreux, méthode des éléments finis mixtes hybrides, stabilité numérique, principe du maximum.

1 Introduction

The ongoing swelling environment problems, in particular the transport of pollutants by underground water, have pressed upon the attention to develop new methods for more precise representative simulations. Subsequently, numerical modeling has played an increasing role to solve such physical processes. Despite the fact that the mathematical models delineating the transport problems are described by coupled systems of nonlinear partial differential equations, in this paper we are restricted to the linear diffusion equation since the focus is to give a numerical study of the approximated solution attained by the MHFE method. Nevertheless, this work is of importance even for the nonlinear advection-diffusion problems since one of the approaches to solve such problems is by using the time splitting operator technique, i.e. advection and dispersion operators are treated separately. Generally, the MHFEM is voted to solve the diffusion part [1].

For the unknown pressure scalar function $p = p(x,t)$ and velocity vector function $u = u(x,t)$, we consider the mass conservation equation and Darcy's law which are given as follows

$$s\,\frac{\partial p}{\partial t} + \nabla.u = f \quad \text{in} \quad \Omega \times (0,T], \tag{1}$$

$$p(x,0) = p^0(x) \quad \text{in} \quad \Omega, \tag{2}$$

$$p = p^D \quad \text{on} \quad \Gamma^D \times (0,T], \tag{3}$$

$$u.\nu = q^N \quad \text{on} \quad \Gamma^N \times (0,T], \tag{4}$$

the so-called Darcy velocity u is given via

$$u = -\mathcal{K}\,\nabla p \quad \text{in} \quad \Omega \times (0,T], \tag{5}$$

where Ω is a bounded domain in R^d $(d = 1,\ldots,3)$ with boundary $\partial\Omega = \Gamma^D \cup \Gamma^N$; $\mathcal{K} = \mathcal{K}(x)$ is the conductivity, it is assumed to be a diagonal tensor with components in $L^\infty(\Omega)$; ν indicates the outward unit normal vector along $\partial\Omega$; $f = f(x,t) \in L^2(\Omega)$ represents the sources; $s = s(x)$ is the storage coefficient; $p^D(x,t)$ and $q^N(x,t)$ are respectively the Dirichlet and Neumann boundary conditions.

It should be noted that the above parabolic, initial boundary value problem can also models many other physical phenomena like heat transfer, chemical transport and electromagnetic current [2]. For the reason of similarity, the fluid flow equation

in porous media is chosen to be studied.

The finite element methods have been the preferred tools over the finite difference methods due to their simple physical interpretation and their flexibility dealing with irregular geometrical domains. In modeling flow in porous media, it is essential to utilize a discretization method which satisfies the physics of the problem, i.e. conserves mass locally and preserves continuity of fluxes. The Raviart-Thomas Mixed Finite Element method of lowest order satisfies these properties. Moreover both the pressure and the velocity are approximated with the same order of convergence (see, e.g., [11, 13]). One of the inconvenient properties of this method is that it leads to an indefinite linear system, so its resolution cannot be achieved by simple robust algorithms like Choleski or Conjugate Gradient methods. Furthermore, the number of unknowns is relatively quite large since both the pressure on each element and the flux through each edge have to be calculated simultaneously [3]. The mixed-hybrid formulation was introduced as an improvement of the MFE where the pressure and the velocity are calculated by solving an equivalent symmetric positive definite linear system. Moreover this technique provides more information about the pressure since degrees of freedom of the pressure on the edges are computed as well.

Numerous works showed the accuracy and the efficiency of this method applied to the stationary diffusion problem [4, 5, 6]. However, numerical comparisons presented in many papers like [7, 8], which showed the upper hand of the MHFEM applied to the parabolic problem with regard to other classical methods, took an implicit supposition of at least one of these two cases: *i)* smooth initial and boundary values, *ii)* sufficient long interval of simulation time $(0, T]$. Discordantly, in this work we show that the MHFEM applied to some particular initial-boundary value diffusion problems leads to relatively erroneous results compared with solutions obtained by the classical FE or FD methods. It is proved that under assumptions of smoothness of initial and boundary conditions, optimal convergence for the pressure and the velocity is obtained (see, e.g., [9, 11, 13]) . In our study here, we show, by numerical experiments, that the theory breaks down if the assumption of smoothness is omitted and no convergence is obtained at some points of large gradient.

The fact that the mixed methods do not obey the discrete maximum principle is well known [11]. In the work presented in [12], it is found that the MHFEM applied to semiconductor device equations violates the discrete maximum principle. This problem is time-independent convection–diffusion problem. However, in this work

we study the MHFEM applied to an groundwater flow problem which is a time-dependent purely diffusive problem.

An outline of the paper is as follows. In the next section, the formulation of the MHFEM corresponding to the Raviart-Thomas space of lowest order is reviewed. Numerical analyses of the solution of an artificial well-posed initial-boundary value problem are discussed in section 3 where we compare the approximated solutions with the exact one. In section 4 we show that, unlike the FD method, the MHFEM conditionally satisfies the discrete maximum principle. Before ending with a conclusion, we give in section 5 some alternative propositions to prevent the non-physical oscillations in the solutions attained by the MHFE method.

2 The mixed-hybrid finite element method

We restrict our discussion to the two-dimensional case, the three-dimensional case follows in a similar manner. The polygonal domain Ω is discretized into a mesh $\mathcal{Q}_h$ consisting of quadrangles or triangles where h denotes the mesh parameter. In practice, quadrangles are restricted to be parallelograms since these can be generated from the reference element by affine transformations. Throughout this paper, we denote by $\mathcal{E}_h$ the set of edges of the grid not belonging to Γ^D, $N_{\mathcal{E}}$ is the cardinal of $\mathcal{E}_h$ and $N_{\mathcal{Q}}$ is the number of discretized elements.

In the mixed finite element method, Darcy's law and the mass conservation equation are approximated individually subsequently, we get additionally the Darcy velocity u as an unknown function. In the following, we present the approximation spaces of our unknowns, the discretization of Darcy's law and that of the mass conservation equation as well as the derived algebraic system to solve.

2.1 Approximation spaces

The essential idea of the MFE methods is to approximate simultaneously the pressure and its gradient. The simplest case of approximation, which is by means of the space of Raviart-Thomas of the lowest order $\mathcal{RT}_0$, will be presented in brief. For more details see [9, 11, 14].

The finite approximation spaces of the pressure p_h and the velocity u_h are the two finite dimensional spaces $\mathcal{M}(\mathcal{Q}_h)$ and $\mathcal{V}(\mathcal{Q}_h)$, respectively.

$\mathcal{M}(\mathcal{Q}_h)$ is the space of piecewise constant function on each element of $\mathcal{Q}_h$, it is given by

$$\mathcal{M}(\mathcal{Q}_h) = \{\varphi \in L^2(\Omega) \mid \varphi/_K \in \mathcal{P}_0(K), K \in \mathcal{Q}_h\},$$

where $\mathcal{P}_d(K)$ is the space of polynomials of total degree d defined on K.

$\mathcal{V}(\mathcal{Q}_h)$ is given by the Raviart-Thomas space $\mathit{RT}_0(\mathcal{Q}_h)$

$$\mathcal{V}(\mathcal{Q}_h) = \mathit{RT}_0(\mathcal{Q}_h) = \{\chi \in L^2(\Omega) \mid \chi/_K \in \mathit{RT}_0(K), K \in \mathcal{Q}_h\},$$

where $\mathit{RT}_0(K)$ stands for the lowest Raviart-Thomas element.

$$\mathit{RT}_0(K) = \begin{cases} \{\phi \in (\mathcal{P}_1(K))^2 \mid \phi = (a + b\,x_1, c + b\,x_2),\ a, b, c \in \mathbb{R}\} & \textit{if } K \textit{ is triangle,} \\ \{\phi \in (\mathcal{P}_1(K))^2 \mid \phi = (a + b\,x_1, c + d\,x_2),\ a, b, c, d \in \mathbb{R}\} & \textit{if } K \textit{ is quadrangle.} \end{cases}$$

The hybridization technique tends to enforce the continuity of the normal component of u_h across the interelement boundaries by using the Lagrange multiplier spaces

$$\begin{array}{lcl} \mathcal{N}(\mathcal{E}_h) & = & \{\lambda \in L^2(\mathcal{E}_h) \mid \lambda/_E \in \mathcal{P}_0(E)\ \ \forall E \in \mathcal{E}_h\}, \\ \mathcal{N}_{g,D}(\mathcal{E}_h) & = & \{\lambda \in \mathcal{N}(\mathcal{E}_h) \mid \lambda = g \text{ on } \Gamma^D\}. \end{array}$$

Now we introduce tp_h a new degree of freedom approximating the traces of the pressure on the edges of the mesh. Thus, the MHFE formulation reads as:
Find $(u_h, p_h, tp_h) \in \mathcal{V}(\mathcal{Q}_h) \times \mathcal{M}(\mathcal{Q}_h) \times \mathcal{N}_{p^D,D}(\mathcal{E}_h)$ such that

$$\begin{cases} \displaystyle\int_\Omega (\mathcal{K}^{-1}\, u_h).\chi_h\, dx + \sum_{K\in\mathcal{Q}_h} \int_{\partial K} tp_h\, \nu_K.\chi_h\, d\ell = \sum_{K\in\mathcal{Q}_h} \int_K p_h \nabla.\chi_h\, dx & \forall\, \chi_h \in \mathcal{V}(\mathcal{Q}_h), \\ \displaystyle\int_\Omega s\frac{\partial p_h}{\partial t}\, \varphi_h\, dx + \int_\Omega \nabla.u_h\, \varphi_h\, dx = \int_\Omega f\, \varphi_h\, dx & \forall\, \varphi_h \in \mathcal{M}(\mathcal{Q}_h), \\ \displaystyle\sum_{K\in\mathcal{Q}_h} \int_{\partial K} u_h.\nu_K\, \lambda_h\, d\ell = \int_{\partial\Omega} q^N\, \lambda_h\, d\ell & \forall\, \lambda_h \in \mathcal{N}_{0,D}(\mathcal{E}_h). \end{cases} \tag{6}$$

2.2 Local basis functions

As a matter of fact, any irregular element K can be mapped from a reference element $\hat{K}$ (as shown in Fig.2.2) by using an affine transformation (see, e.g., [9, 10, 14]). This mapping is defined as

$$\begin{array}{lcl} \hat{K} & \longmapsto & K \\ \hat{x} & \longmapsto & x = T_K\hat{x} + b_K \end{array}$$

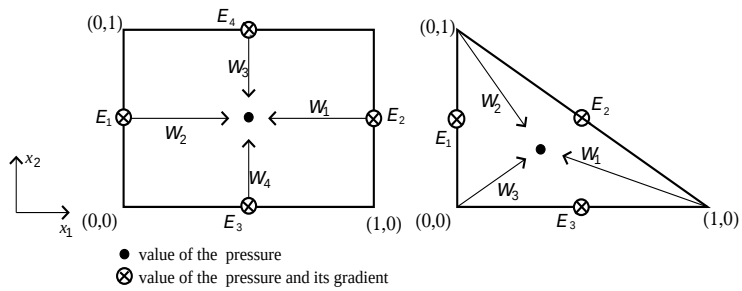

Figure 1: The approximated unknowns and the basis functions on the reference elements.

Subsequently, $\mathcal{V}(K) = RT_0(K)$ could be written as

$$\mathcal{V}(K) = \frac{1}{J_K} T_K \mathcal{V}(\hat{K}),$$

where T_K is the transformation matrix, $J_K = \det(T_K)$ is the Jacobian and b_K is a point in K.
The Raviart-Thomas basis functions of $\mathcal{V}(\hat{K})$, defined on the reference element, are given by If K is a triangle (as depicted in Fig.2.2), a choice for a basis of the 3-dimensional space $\mathcal{V}(\hat{K})$ is

$$\hat{w}_{\hat{K},E_1} = \begin{bmatrix} \hat{x}_1 - 1 \\ \hat{x}_2 \end{bmatrix}, \ \hat{w}_{\hat{K},E_2} = \begin{bmatrix} \hat{x}_1 \\ \hat{x}_2 - 1 \end{bmatrix}, \ \hat{w}_{\hat{K},E_3} = \begin{bmatrix} \hat{x}_1 \\ \hat{x}_2 \end{bmatrix}. \tag{7}$$

One the other hand, if K is a rectangle (see Fig.2.2), $\mathcal{V}(\hat{K})$ becomes a 4-dimensional space with the basis functions

$$\begin{aligned} \hat{w}_{\hat{K},E_1} &= \begin{bmatrix} \hat{x}_1 - 1 \\ 0 \end{bmatrix}, \ \hat{w}_{\hat{K},E_2} = \begin{bmatrix} \hat{x}_1 \\ 0 \end{bmatrix}, \\ \hat{w}_{\hat{K},E_3} &= \begin{bmatrix} 0 \\ \hat{x}_2 - 1 \end{bmatrix}, \ \hat{w}_{\hat{K},E_4} = \begin{bmatrix} 0 \\ \hat{x}_2 \end{bmatrix}. \end{aligned} \tag{8}$$

One can easily verify that for every $\chi_K = \sum_{E \subset \partial K} q_{K,E}\, w_{K,E} \in \mathcal{V}(K)$ and $K \in \mathcal{Q}_h$, the following properties are satisfied.

1. $\nabla.\chi_K$ is constant over K
2. $\nu_{K,E}.\chi_K = q_{K,E}$ is constant on each $E \subset \partial K$

Hence u_K is uniquely determined by the normal fluxes $q_{K,E} = u_K.\nu_{K,E}$ on the edges of K, where $\nu_{K,E}$ denotes the outer normal vector on E with respect to K.

2.3 Approximation equations

The finite dimensional space $\mathcal{V}(\mathcal{Q}_h)$ is spanned by linearly independent vectorial basis functions $w_{K,E}$, $E \subset \partial K$, $K \in \mathcal{Q}_h$, such that $w_{K,E}$ has its support in K ($supp(w_{K,E}) \subseteq K$) and

$$\int_{E'} w_{K,E}.\nu_K \, d\ell = \delta_{EE'}, \quad E, E' \subset \partial K.$$

These functions can be chosen the local bases functions given in (7) or (8). Thus, a function $u_h \in \mathcal{V}(\mathcal{Q}_h)$ has three degrees of freedom per element which are the fluxes across the element's edges

$$u_h(x) = \sum_{K \in \mathcal{Q}_h} \sum_{E \subset \partial K} q_{K,E} \, w_{K,E}(x), \; x \in \Omega.$$

The two space $\mathcal{M}(\mathcal{Q}_h)$ and $\mathcal{N}(\mathcal{E}_h)$ are spanned respectively by the linearly independent scalar basis functions φ_K, $K \in (\mathcal{Q}_h)$, and λ_E, $E \in (\mathcal{E}_h)$, such that

$$\begin{aligned} \varphi_K(x) &= \delta_{K,K'}, \; x \in K', \quad K, K' \in \mathcal{Q}_h, \\ \lambda_E(x) &= \delta_{E,E'}, \; x \in E', \quad E, E' \in \mathcal{E}_h. \end{aligned}$$

Thus, a function $p_h \in \mathcal{M}(\mathcal{Q}_h)$ (resp. $tp_h \in \mathcal{N}(\mathcal{E}_h)$) has one degree of freedom of constant value per element $K \in \mathcal{Q}_h$ (resp. $E \in \mathcal{E}_h$), such that

$$\begin{aligned} p_h(x) &= \sum_{K' \in \mathcal{Q}_h} p_{K'} \, \varphi_{K'}(x) = p_K, \quad x \in K, \\ tp_h(x) &= \sum_{E' \in \mathcal{E}_h} tp_{E'} \, \lambda_{E'}(x) = tp_E, \quad x \in E. \end{aligned}$$

Now, we individually investigate the underlying equations in (6), which can be integrated over the element level.

2.3.1 Discretization of Darcy's law

By taking as test functions χ_K successively the basis functions $w_{K,E}$, the discretized equation of Darcy's law (the first equation in (6)) becomes

$$\int_K (\mathcal{K}_K^{-1}\, u_K).\chi_K dx + \sum_{E\subset\partial K} \int_E tp_{K,E}\, \chi_K.\nu_{K,E} d\ell = \int_K p_K \nabla.\chi_K dx, \tag{9}$$

where $\mathcal{K}_K$ is a piecewise approximation of the conductivity tensor over K, and

$$tp_E = tp_{K,E} = \begin{cases} tp_{K',E} & if\ E = K\cap K' \\ p_E^D & if\ E\in\Gamma^D \end{cases}, \quad E\in\mathcal{E}_h\cup\Gamma^D,\ \ K,\, K'\in\mathcal{Q}_h.$$

By integrating (9) and by making use of the Raviart-Thomas space basis properties, the following equations come into view

$$\sum_{E'\subset\partial K} (B_K)_{E,E'}\, q_{K,E'} = p_K - tp_{K,E}, \qquad E\subset\partial K,\ K\in\mathcal{Q}_h. \tag{10}$$

In the matrix form, (9) is written as

$$B_K\, Q_K = p_K\, e - T_{P_K}, \qquad K\in\mathcal{Q}_h, \tag{11}$$

where

Q_K and T_{P_K} are N_K- dimensional vectors containing respectively the fluxes $q_{K,E}$ and the traces of the pressure $tp_{K,E}$ on each $E\subset\partial K$, with N_K is the number of edges of K ;

e refers to the elementary divergence vector. It is of dimension N_K and unitary entries;

B_K is a $N_K\times N_K$ symmetric positive definite matrix whose elements are

$$(B_K)_{E,E'} = \int_K w_{K,E}^T\, \mathcal{K}_K^{-1}\, w_{K,E'}\, dx. \tag{12}$$

It should be noted that these integrations are all evaluated exactly.

The last equation in (6) is equivalent to

$$\begin{aligned} &\int_E u_K.\nu_{K,E}\, d\ell + \int_E u_{K'}.\nu_{K',E}\, d\ell = 0 && if \quad E = K\cap K', \\ &\int_E u_K.\nu_{K,E}\, d\ell = q_E^N && if \quad E\in\Gamma^N, \end{aligned}$$

where $q_E^N = \int_E q^N \, d\ell$.
Hence, the normal components of u_h are continuous across the interelement boundaries, i.e.

$$q_{K,E} = \begin{cases} -q_{K',E} & if\ E = K \cap K', \\ q_E^N & if\ E \in \Gamma^N. \end{cases} \tag{13}$$

By inverting the matrix B_K and using (13), it is possible to eliminate the unknown flux. As a result, the reduced algebraic system, acquired by discretizing Darcy's law with unknowns the pressure head given in P and its traces in T_P, becomes

$$R^T P - M T_P + V = 0, \tag{14}$$

where

R^T is the transpose matrix of R which is a sparse matrix of dimension $N_{\mathcal{E}} \times N_{\mathcal{Q}}$ with nonzero elements given by

$$(R)_{K,E} = \alpha_{K,E} = \sum_{E' \subset \partial K} (B_K^{-1})_{E,E'}, \quad E \subset \partial K;$$

M is a $N_{\mathcal{E}} \times N_{\mathcal{E}}$ sparse matrix with nonzero entries defined as

$$(M)_{E,E'} = \sum_{\partial K \supset E,E'} (B_K^{-1})_{E,E'};$$

V is a $N_{\mathcal{E}}$–dimensional vector corresponding to the Dirichlet and Neumann boundary conditions.

2.3.2 Discretization of the mass conservation equation

By integrating the mass conservation equation (the second equation in (6)) where the test functions ϕ_h are successively replaced by the basis functions of $\mathcal{M}$, we get

$$s_K \mu_K \frac{\partial p_K}{\partial t} + \sum_{E \subset K} q_{K,E} = f_K \qquad K \in \mathcal{Q}_h, \tag{15}$$

where s_K and f_K are respectively the approximations of the storage coefficient and the sink/source term over K, μ_K denotes the measure of K.
Therefrom, by using (11) to replace the sum of fluxes in (15), we obtain an ordinary differential system which is given in its matrix form

$$S \frac{dP}{dt} + D P - R T_P = F, \tag{16}$$

where

S is a $N_{\mathcal{Q}} \times N_{\mathcal{Q}}$ diagonal matrix with entries $(S)_{K,K} = \mu_K \, s_K$;

D is also a $N_{\mathcal{Q}} \times N_{\mathcal{Q}}$ diagonal matrix whose coefficients are

$$(D)_{K,K} = \alpha_K = \sum_{E \subset \partial K} \alpha_{K,E} \, ;$$

F is a vector of dimension $N_{\mathcal{Q}}$, it corresponds to the source/sink function as well as to the imposed pressure given by the Dirichlet boundary conditions.

2.4 The derived algebraic system

The spatial discretization of the governing equations obtained by applying the mixed-hybrid formulation led to two systems. The first one, given in (14), is an algebraic system of unknowns P and T_P and the second is an ordinary system of first order differential equations in time (16). By inverting the matrix M which is symmetric, positive definite [3, 14, 15], it is possible to eliminate T_P from (16) and consequently a stiff initial value problem is attained

$$\begin{cases} \dfrac{dP}{dt} & = & LP + W, \\ P(0) & = & P^0, \end{cases} \tag{17}$$

where

$$L = -S^{-1}(D - R^T M^{-1} R), \; W = R^T M^{-1} V + F.$$

The semi-exact solution (solution of the problem discretized in space with exact time integral operator) of (17) is given by the following formula

$$P(t) = e^{tL} P^0 + \int_0^t e^{(t-s)L} \, W ds. \tag{18}$$

For simplicity, we assume that p^D, q^N and f are time independent piecewise constant functions over the grid then W is time independent and so (18) turns into

$$P(t) = e^{tL}(P^0 + L^{-1} W) - L^{-1} W \qquad t \in [0, T]. \tag{19}$$

This solution is computationally high-priced due to the difficulties in evaluating the exponential besides inverting the matrix M. To avoid such problem, a temporal discretization of the differential operator in (16) is indispensable. Nevertheless, the solution given in (19) will be useful in appraising the accuracy of the time-discretization

scheme. Since our primary motivation here is orientated to study the non-physical oscillations in the approximated pressure which is caused by the spatial discretization (as we will see later), a first order accurate scheme for time-discretization is adequate. Accordingly, the classical Euler backward (implicit) method is elected for the reason that it is unconditionally stable besides it is easy to be carried out.

We subdivide $[0, T]$ into a finite number of equal subintervals of time steps Δt. By replacing the differential time operator in (16) by the difference quantity $(P^n - P^{n-1})/\Delta t$ then by simple substitution of P^n in (14), the following system is achieved

$$\begin{cases} (M - \Delta t N)\, T_P^n = R\, G^{-1}\, (S\, P^{n-1} + \Delta t F) + V \\ G\, P^n = S P^{n-1} + \Delta t R^T T_P^n + \Delta t F \end{cases} \tag{20}$$

where $G = S + \Delta t D, \;\; N = R G^{-1} R^T$.

Hence the problem is reduced to compute, at every time step, first T_P by solving a linear system with symmetric, positive definite coefficient matrix $(M - \Delta t N)$ [15], then P by solving a diagonal linear system. As a matter of fact, experimental inspections showed the adaptability and the robustness of the preconditioned conjugate gradient method in solving such systems [10].

3 Presentation of the problem

Generally, The MHFE method is a wildly used tool to solve linear diffusion equations specially when both the pressure and the velocity of the flow are needed to be approximated. As a matter of fact, numerical laboratory works with this method furnished many phenomena where non-physical solutions are obtained and which are still inexplicable due to the complication of the initial-boundary values or the complexity of the underlying geometrical regions. For a better understanding of the problem, in this section we present a very simple well-posed initial-boundary value problem whereto various comparisons and observations of the numerical solution behavior are interpreted.

The domain Ω is taken to be of rectangular shape $(0, 20) \times (0, 10)$ with the fol-

lowing initial-boundary conditions.

$$\begin{cases} s\,\dfrac{\partial p}{\partial t} + \nabla.u = 0 & \text{in} \quad \Omega \times (0,T] \\ u = -\mathcal{K}\,\nabla p & \text{in} \quad \Omega \times (0,T] \\ p(x,0) = 0 & \text{in} \quad \Omega \\ p = 1 & \text{on} \quad \Gamma_1^D \times (0,T] \\ p = 0 & \text{on} \quad \Gamma_2^D \times (0,T] \\ u.\nu = 0 & \text{on} \quad \Gamma^N \times (0,T] \end{cases} \tag{21}$$

where Γ_1^D, Γ_2^D are respectively the left and the right hand perpendicular sides of the domain, $\Gamma_1^D = \{0\} \times [0,10]$, $\Gamma_2^D = \{20\} \times [0,10]$ and $\Gamma^N = \partial\Omega \backslash \Gamma^D$.

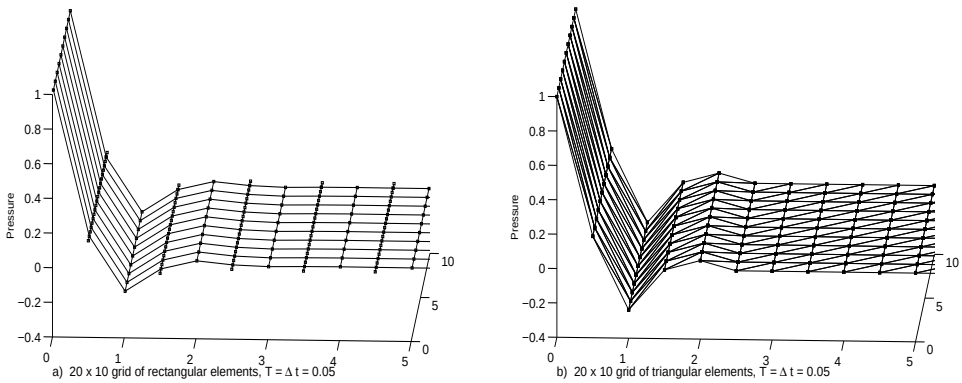

Figure 2: The pressure and its traces over the grid.

We discretize Ω into a (20×10) uniform grid, the macro-elements are either rectangles or right angle triangles . In Fig.2, both together, the pressure P and its traces T_P are simulated over the grid with time step $\Delta t = T = 0.05$, $s = 1$ and $\mathcal{K} = 1$. It is clear that the two spatial discretization lead to severe peaks at some points of the solution. These oscillations cannot be evaded or disregarded since they even cause large critical deviations in the direction of the flow velocity, as appears in Fig.3. Even though this sample problem can be considered as a one-dimensional problem since physically the flow diffuses horizontally, the non horizontal deviations of the flow velocity appearing in Fig.3b justify why the problem is discretized in the two dimensional space. However, for the sake of clearness, in the runs the pressure will be visualized with one variable in space.

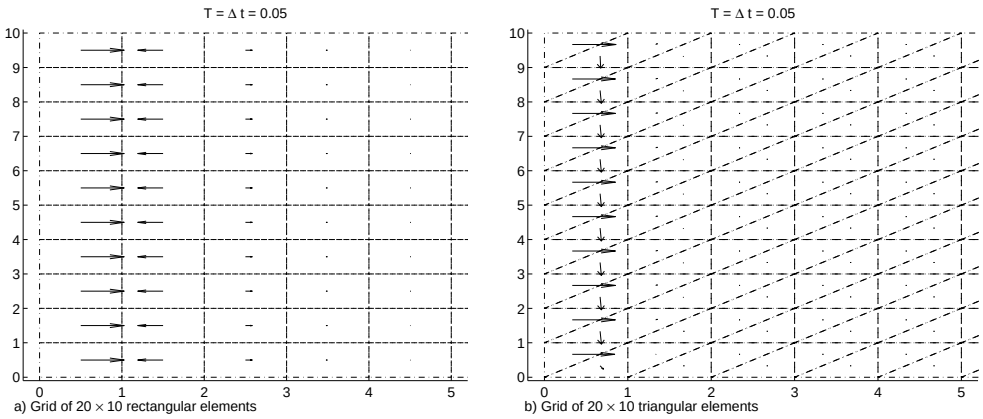

Figure 3: The velocity of the flow at the center of every element.

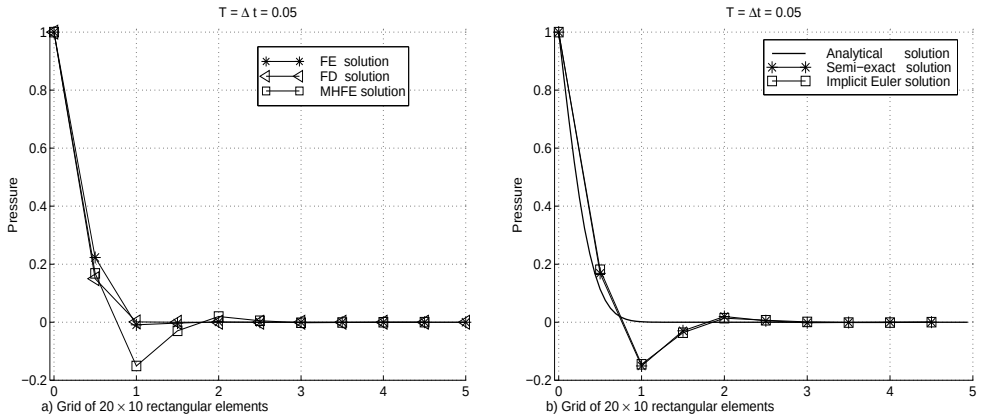

Figure 4: Comparisons between the analytical solution and the approximated solutions.

In Fig.4a we compare the approximated solutions of (21) obtained by applying the MHFE, FE and FD methods. We find that oscillatory solution is also obtained by the FE method except that these oscillations stay small compared to those obtained by the MHFEM. On the other hand, the finite difference method achieves a numerical solution free from any oscillations.

For an infinite long geometrical domain Ω, the analytic solution of (21) is given by (see [16])

$$p(x,t) = p^D erfc\left(\frac{x}{2\sqrt{t}}\right), \qquad (x,t) \in [0,\infty) \times [0,\infty), \tag{22}$$

where

$$erfc(\nu) = 1 - \frac{2}{\sqrt{\pi}} \int_0^{\nu} e^{-x^2}\, dx, \qquad \nu \in \mathbb{R}.$$

By comparing the analytical solution (22), the semi-discretized time-dependent solution (19) and the Euler backward solution (20), as depicted in Fig.4b, the following remarks are deduced.

- the sharp layer appearing in the analytic solution restricts its smoothness.
- dis-convergences in the approximated solution occur in the region where large gradients in the analytical solution are located.
- the semi-exact solution is also oscillatory moreover, it behaves in a similar manner as the Euler backward solution.

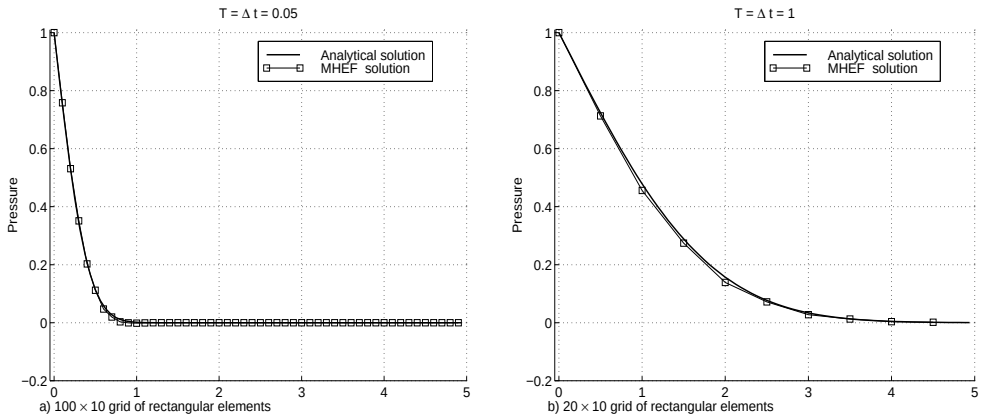

Figure 5: Reduction of space-step or enlargement of time interval wipes out oscillations.

Since, in general, any discretizing scheme in time attempts to converge to the exact time dependent solution, no time-discretizing method is able to amend these oscillations. Furthermore, if smaller time steps are taken the results may be even worse.

Reasonably, we focus on the spatial decomposition of the domain. For the moment we try a uniform refinement of the mesh by taking a (100×10) grid. Depicted results in Fig.5a show that the MHFE method leads to an acceptable approximation of the exact solution. However by trying out smaller time step, oscillations will reappear again.

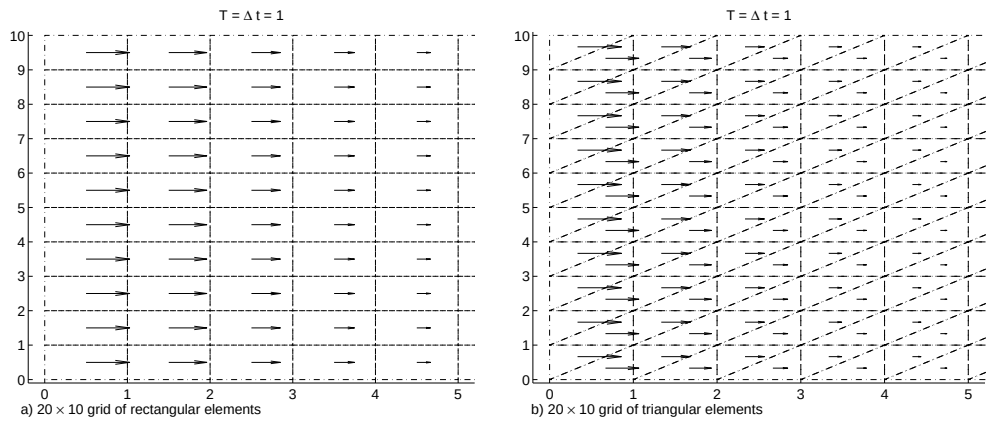

Figure 6: The velocity of the flow at the center of every element.

One more numerical test which will help to clarify this phenomenon is by increasing the simulation time interval $[0, T]$. In Fig.5b, even though without any refinement of the mesh, convergence of the approximated pressure (similarly its derivative Fig.6) is attained and this is due to the intuitive nature of linear diffusion process whose solution becomes smoother as t increases. It should be noted that similar oscillatory solutions may be also obtained if the sink/source function $f(x, t)$ varies abruptly in time.

As a primary conclusion, it becomes obvious to mind that in order to prevent any non-physical solutions it is advantageous to vary the mesh size in time and space according to the smoothness of the analytic solution. In the sequence, a criterion relating the temporal and spatial steps is presented whereby the domain can be discretized with maximum space steps and without oscillations in the solution.

4 Discrete maximum principle

The maximum principle is generally used to explore some information about the theoretical solution of some types of PDE. Specifically, it asserts that the solution cannot have a maximum or a minimum within the interior of the underlying domain besides, it is employed to show that the solution of certain problems must be non-negative. Accordingly, by applying the maximum principle to the problem given in (21), we obtain the following (see, e.g., [17, 18])

$$\begin{array}{lrcl} \textbf{i.} & \max\limits_{\bar{\Omega}\times(0,T]} \{p(x,t)\} & \leq & \max\limits_{\partial\Omega\times(0,T]} \{p(x,t),0\} \\ \textbf{ii.} & \min\limits_{\bar{\Omega}\times(0,T]} \{p(x,t)\} & \geq & \min\limits_{\partial\Omega\times(0,T]} \{p(x,t),0\} \end{array} \tag{23}$$

where $\bar{\Omega} = \Omega \cup \partial\Omega$.

So the pressure solution cannot have negative values as well as it is restricted between the Dirichlet boundary values. In the sequence, we verify whether the discrete maximum principle is obeyed by the discretized scheme given in (20) and this by investigating the following two properties:

$$\textbf{1.} \quad T_P^{n-1} \geq 0 \Longrightarrow T_P^n \geq 0 \tag{24}$$

$$\textbf{2.} \quad \max(T_P^n) \leq \max(T_P^{n-1}) \tag{25}$$

We shall investigate the positivity of the scheme locally over each macro-element, i.e. $tp_{K,E}^{n-1} \geq 0 \Rightarrow tp_{K,E}^{n} \geq 0$ for $E \in \mathcal{E}_h, K \in \mathcal{Q}_h$. For the sake of simplicity, we shall introduce the case of uniform rectangular discretization of the mesh over homogenous isotropic medium such that $\mathcal{K} = aI, s = s_K \quad \forall K \in \mathcal{Q}_h$, where a is the anisotropic coefficient and I is the 2×2 identity matrix.

In Fig.7 we consider any two arbitrary adjacent elements in $\mathcal{Q}_h$. The local mass conservation property enables us to rewrite the mixed-hybrid formulation over each element $K = K_1,\ K_2$. By inverting B_K in (11) furnished from Darcy's law discretization, we get

$$q_{K,E} = a\left(\alpha_{K,E}\, p_K - \sum_{E'\subset\partial K} (B_K^{-1})_{E,E'}\, tp_{K,E'}\right) \quad \forall\, E \subset \partial K,\ K = K_1,\, K_2 \tag{26}$$

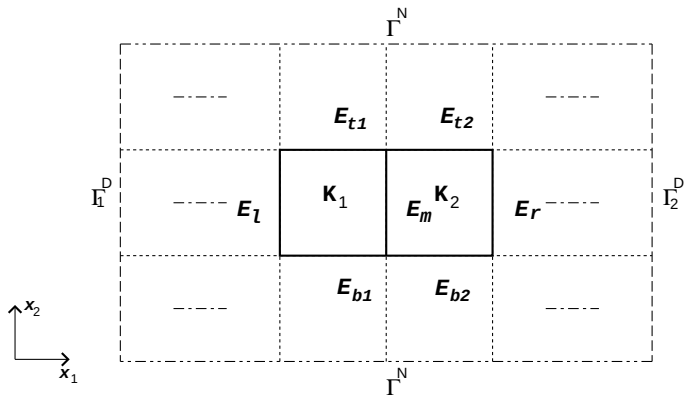

Figure 7: Two arbitrary adjacent element with their corresponding edges.

B_K can be simply obtained by exact integrations over each element K, its inverse is given by

$$B^{-1} = B_K^{-1} = 2 \begin{pmatrix} 2\frac{\Delta x_2}{\Delta x_1} & \frac{\Delta x_2}{\Delta x_1} & 0 & 0 \\ \frac{\Delta x_2}{\Delta x_1} & 2\frac{\Delta x_2}{\Delta x_1} & 0 & 0 \\ 0 & 0 & 2\frac{\Delta x_1}{\Delta x_2} & \frac{\Delta x_1}{\Delta x_2} \\ 0 & 0 & \frac{\Delta x_1}{\Delta x_2} & 2\frac{\Delta x_1}{\Delta x_2} \end{pmatrix} \tag{27}$$

From the spatial and temporal discretization of the mass conservation equation, we obtain

$$p_K^n = p_K^{n-1} - \frac{\Delta t}{s\mu} \sum_{E \subset \partial K} q_{K,E}^n \ , \qquad K = K_1,\, K_2. \tag{28}$$

Since there is no vertical diffusion of the flow, we have null fluxes across the horizontal edges, i.e.

$$q_{E_{t1}} = q_{E_{b1}} = q_{E_{t2}} = q_{E_{b2}} = 0 \tag{29}$$

As depicted in Fig.7, the labels l, r, t, b and m refer to left, right, top, bottom and middle edges, respectively. Now by enforcing the continuity of the flux through the middle edge and by eliminating the unknowns $q_{K,E}$ (substitute (29) and (26) in (28)), the following system is achieved

$$c_1\, tp_{E_m}^n = c_2\, (tp_{E_l}^n + tp_{E_r}^n) + c_3\, (p_{K_1}^{n-1} + p_{K_2}^{n-1}) \tag{30}$$

$$\left\{\begin{array}{l} p^n_{K_1} = \dfrac{1}{1+2\lambda}\, p^{n-1}_{K_1} + \dfrac{\lambda}{1+2\lambda}\,(tp^n_{E_l} + tp^n_{E_m}) \\ p^n_{K_2} = \dfrac{1}{1+2\lambda}\, p^{n-1}_{K_2} + \dfrac{\lambda}{1+2\lambda}\,(tp^n_{E_m} + tp^n_{E_r}) \end{array}\right. \tag{31}$$

where
$\mu = \Delta x_1\, \Delta x_2$, $\alpha = \sum_{i=1,4} B^{-1}_{i,1} = 6\frac{\Delta x_2}{\Delta x_1}$, $\lambda = \frac{a\alpha\Delta t}{s\mu}$, $c_1 = (B^{-1}_{11} + B^{-1}_{22} - \frac{2\,\alpha\lambda}{1+2\lambda})$, $c_2 = (\frac{\alpha\lambda}{1+2\lambda} - B^{-1}_{21})$ and $c_3 = \frac{\alpha}{1+2\lambda}$.

It is easily to verify that c_1 and c_3 are always nonnegative, whereas c_2 is conditionally positive.

Proposition 4.1 *The discrete maximum principle is satisfied by the MHFEM if c_2 is nonnegative, i.e.*

$$c_2 \geq 0 \Longleftrightarrow \frac{\Delta x_1^2}{\Delta t} \leq \frac{6a}{s}.$$

Proof:

To verify the positivity of the scheme, the classical mathematical induction technique is utilized. We suppose that $tp^{n-1}_{K,E}$, $p^{n-1}_K \geq 0$ and let's prove that $tp^n_{K,E}$, $p^n_K \geq 0$ $\forall K \in \mathcal{Q}_h$, $E \in \mathcal{E}_h$.

We denote by $\mathcal{E}^\perp$ the set of vertical edges of the mesh and $E_m \in \mathcal{E}^\perp$ such that

$$tp^n_{E_m} = \min\{tp^n_{K,E} \mid E \in \mathcal{E}^\perp,\ K \in \mathcal{Q}_h\}.$$

We shall only consider the non trivial case, i.e. $E_m \notin \Gamma^D$. So E_m can be considered as a interior edge (suppose $E_m = K_1 \cap K_2$). Consequently, by applying (30), we get

$$\begin{array}{rcll} c_1\, tp^n_{E_m} & = & c_2\,(tp^n_{E_l} + tp^n_{E_r}) + c_3\,(p^{n-1}_{K_1} + p^{n-1}_{K_2}) & \\ & \geq & 2\,c_2\, tp^n_{E_m} + c_3\,(p^{n-1}_{K_1} + p^{n-1}_{K_2}) & (c_2, c_3 \geq 0). \end{array}$$

Since $(c_1 - 2\,c_2) \geq 0$ and p^{n-1}_K are positive by our assumption then $tp^n_{E_m} \geq 0$ and by making use of (31), one can deduce the positivity of p^n_K for all $K \in \mathcal{Q}_h$. Now, if E is a horizontal edge in $\mathcal{E}_h$ then one can easily deduce from (26) and (29) that $tp^n_{K,E}$ and p^n_K have the same sign. Therefore, the positivity of the

scheme holds. In order to avoid boring repetitions, similar technique can be used to verify the second property given in (25) by taking

$$tp^n_{E_m} = \max\{tp^n_{K,E} \mid E \in \mathcal{E}^{\perp},\ K \in \mathcal{Q}_h\}.$$

□

In should be noted that one can get the same results by verifying that the coefficient matrix $(M - \Delta t\, N)$ an M–matrix. Since this matrix is symmetric definite positive then the M–matrix property holds by showing that the off-diagonal entries are non-positive ([20]). As a result, in the general case of rectangular or uniform triangular grids, the MHFEM obeys the discrete maximum principle if the following criteria are satisfied for every $K \in \mathcal{Q}_h$

$$\begin{array}{rcll} \dfrac{(\Delta x_1^2)_K}{\Delta t} & \leq & \dfrac{6\, a_K}{s_K} & \textit{if } K \textit{ is a rectangle,} \\ \dfrac{(\Delta x_1^2)_K}{\Delta t} & \leq & \dfrac{6\, a_K}{\sqrt{2}\, s_K} & \textit{if } K \textit{ is a triangle.} \end{array} \tag{32}$$

The above criteria have a physical signification since the fraction $\dfrac{a_K}{s_K}$ $(\mathrm{L}^2\,\mathrm{T}^{-1})$ is the so-called the *diffusivity coefficient* [19]. Therefore, by logical inference, the space steps must not be larger than the *displacement pressure* in order to prevent negative solutions. It should be noted that similar criteria are also obtained in the case of standard Galerkin method however, numerical experimentations showed that the non-physical oscillations obtained by this method are relatively less significance than those obtained by the MHFE method (see Fig.4). On the other hand, the classical finite difference method with one nodal degree of freedom seeks the approximated pressure by solving of the form a symmetric, definite positive penta-diagonal linear system. Hereby, one can easily verify that the discrete maximum principle is unconditionally obeyed by showing that coefficient matrix is an M–matrix (see [21]).

5 Various alternative approaches to prevent oscillations

5.1 Refinement

The global refinement is maybe the simplest technique in order to enhance the accuracy of the approximated solution. As we have seen above, the criteria given in (32) enable us to refine the grid with maximum space steps (see Fig.8).

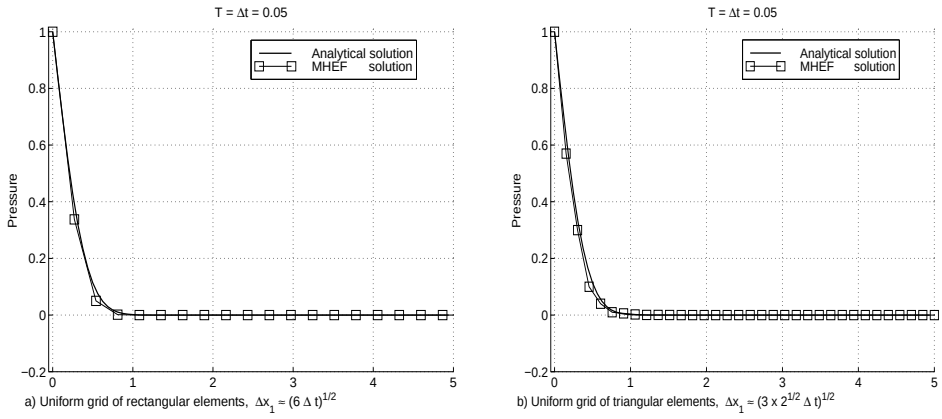

Figure 8: Global refinement of the grid by using the maximum allowed space step.

Although speed and storage capabilities of computers have recently improved, the ever increasing demand to more time and memory requirements is endless. Due to such circumspections, the global refinement technique may not be preferred in sizable problems.

5.2 Adaptive techniques

In general, two types of adaptive techniques are mostly used; the first one is the local refinement method whereby uniform fine grids are added in the regions where the approximated solution lacks adequate accuracy, and the second is the moving mesh technique where nodes are relocated at necessary time steps.
We have found that the adaptive techniques could ameliorate the correctness of the solution despite the fact that their idea may not fit in with the conditions of the discrete maximum principle. However, we can define a process so that the discrete maximum principle is satisfied locally and precisely in the regions where high oscillations occur. Thereafter, we follow a similar work presented in [23] where the mesh is moved so that a predetermined estimated error is satisfied and a system of differential equations is used to dominate the locations of the nodes. In our procedure, the error estimates rely on the properties given in (23) and the criteria previously discussed in (32) control the motion of the elements. Thus, we regroup the nodes (or add new nodes) in the regions where the solution behaves sharply in so that (32) are satisfied. However, in order to avoid non-smooth or coarse meshes,

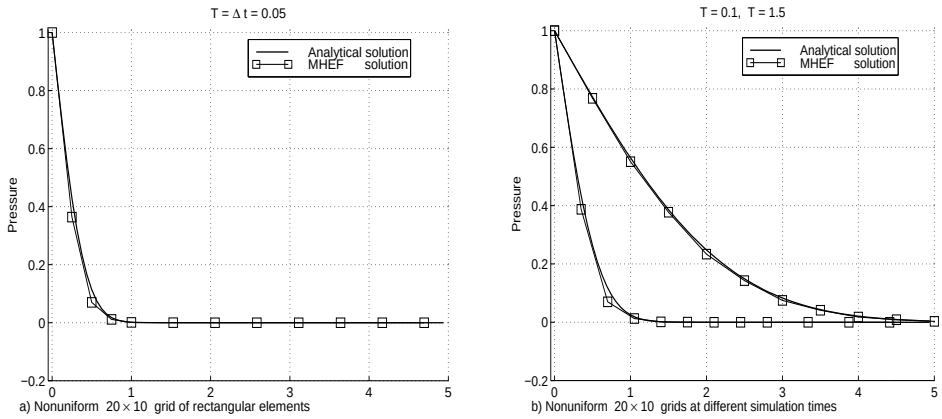

Figure 9: Relocating the mesh nodes at each time step .

we uniformly redistribute the other nodes. By comparing figures 4 and 9a, one can clearly notice the improvement in the approximated solution achieved by the redistribution of the nodes. In Fig.9b, we present the MHFE solution at different time simulations. It should be noted that the requisite solution with respect to the original grid can be simply obtained by linear interpolations.

5.3 Lumped-Mass method

By using the integration formula proposed in [22, 3] for rectangular elements and in [24] for acute triangulations (the angles of triangular elements $\leq \pi/2$), the elementary matrix B_K boils down to a diagonal matrix and so is M. Then the off-diagonal entries of $(M - \Delta t N)$ are

$$(M - \Delta t N)_{E,E'} = -\Delta t (R G^{-1} R^T)_{E,E'} \leq 0 \quad \forall\, E \neq E',\ E, E' \subset \mathcal{E}_h.$$

Therefore, the coefficient matrix $(M - \Delta t N)$ is an M-matrix.

Conclusion

The mixed-hybrid finite element method has been developed to handle many physical models where the classical numerical methods such as the finite element or the finite difference methods fail to give satisfactory representative approximations. The

superior properties of this method is that it allows to conserve mass locally besides the primary unknown and its derivative are approximated simultaneously. In this work we have introduced a brief review of the MHFE formulation corresponding to the lowest order Raviart-Thomas space which is the most popular. Due to the fact that the MHFEM does not obey the discrete maximum principle, many numerical experiments have brought to light some phenomena where non-physical oscillations are obtained. Accordingly, we have clearly seen such oscillations in the approximated solution of a simple artificial initial-boundary value problem by using rectangular and triangular grids. Consequently, a diffusivity criterion relating the space and time steps is given with respect to both spatial discretization (rectangular and triangular grids). Some alternative solutions are suggested to solve this difficulty. The first natural remedy is a global or local refinement of the grid where we refine the mesh at necessary time steps in a way that we regroup the nodes in the regions where fast changes in the solution occur. The second idea is to use the mass-lumping technique whereby integrations are evaluated by using some approximation formula. Such techniques enable to reduce the MHFE method to the finite difference or finite volume methods and in both cases the discrete maximum principle is obeyed.

References

[1] Ph. Ackerer, A. Younes and R. Mose. Modeling Variable Density Flow Transport in Porous Medium: 1. Numerical Model and Verification.. *Transport in Porous Media*, 1998; 1350:1–29.

[2] G. Yeh. *Computational Subsurface Hydrology: Fluid Flows.* Kluwer Academic Publishers. The Pennsylvania State University, 1999.

[3] G. Chavent and J-E. Roberts. A unified physical presentation of mixed, mixed-hybrid finite element method and standard finite difference approximations for the determination of velocities in water flow problems. *Adv. Water Resour.*, 1991; **14**(6): 329–348.

[4] T. Arbogast, M. Wheeler and I. Yotov. Mixed Finite Elements for Elliptic problems with Tensor Coefficients as Cell-Centered Finite Differences. *SIAM J. Numer. Anal.*, 1997;**34**(2):828–852.

[5] M. Nakata, A. Weiser and M. Wheeler. Some superconvergence results for mixed finite elements for elliptic problems on rectangular domains. *The Math. of Finite Elements and Applications*, Academic Press, London, 1985; 367–389.

[6] J-P. Hennart. Nodal Schemes, Mixed-Hybrid finite elements and Block-Centered Finite Differences. *Rapport de Recherche INRIA*, 1985; N° 386.

[7] R.Mose, P. Siegel, Ph. Ackerer and G. Chavent. Application of the mixed-hybrid finite element approximation in a ground water flow model: Luxury or necessity?. *Water Resour. Res.*, 1994; **30**(11):3001.

[8] L. Durlofsky. Accuracy of mixed and control volume finite element approximations to Darcy velocity and related quantities. *Water Resour. Res.*, 1994; **30**(4):965.

[9] J. Thomas. *Sur l'Analyse Numérique des Méthodes d'Elément Finis Hybrides et Mixtes.* Thèse de Doctorat d'Etat, Univ. de Pierre et Marie Curie, 1977.

[10] E. Kaasschieter and A. Huijben. Mixed-Hybrid Finite Elements and streamline Computation for the Potential Flow Problem. *TNO Institute of Applied Geoscience*, 1990; TNO–Report PN 90-02-A.

[11] F. Brezzi and M. Fortin. *Mixed and Hybrid Finite Element Method*, 1991; Springer-Verlag, New York.

[12] F. Brezzi, L. Marini and P. Pietra. Two-dimensional Exponential fitting and applications to Drift-Diffusion Models. *SIAM J. Numer. Anal.*, 1989; **26**(6):1342–1355.

[13] I. Yotov. *Mixed Finite Element Methods for Flow in Porous Media.* Ph.D thesis, Univ. of Texas, 1996.

[14] G. Chavent and J. Jaffré. *Mathematical Models and Finite Elements for Reservoir Simulation.* Elsevier Science Publishers B.V, Netherlands, 1986.

[15] H. Hoteit, J. Erhel and R. Mosé. Numerical reliability and time requirements for the mixed methods applied to flow problems in porous media. (in preparation).

[16] H. Carslaw and J. Jaeger. *Conduction of Heat is solids.* Claredon, Oxford, 1959;363–365.

[17] M. Protter and H. Weinberger. *Maximum Principles in Differential Equations.* Prentice-Hall Partial Differential Equations Series, New Jersey.

[18] M.Renardy and R. Rogers. *An Introduction to Partial Differential Equations.* Springer-Verlag, New York.

[19] G. Marsily. *Hydrogéologie Quantitative*, 1981; Masson, Paris.

[20] Gunther Windisch. *M–matrices in Numerical Analysis*, 1989; Teubner-Texte zur Mathematik:115.

[21] G. Amiez and P. Gremand. On a numerical approach of Stefan-like problems. *Numer. Math.*, 1991; **59**:71–89.

[22] T. Russell and M. Wheeler. Finite element and finite difference methods for continuous flows in porous media . *SIAM* , R. Ewing, The Mathematics of Reservoir Simulation, 1983; 35–106.

[23] S. Adjerid and J. Flaherty. A moving finite element method with error estimation and refinement for one-dimensional time dependent partial differential equations. *SIAM J. Numer. Anal.*, 1986; **23**(4):778–796.

[24] J. Baranger, J. F. Maitre and F. Oudin. Convection between Finite Volume and Mixed Finite Element Methods. *Equipe d'analyse Numerique Lyon Saint-Etienne*, 1995; N° 198.

Unité de recherche INRIA Rennes
IRISA, Campus universitaire de Beaulieu - 35042 Rennes Cedex (France)

Unité de recherche INRIA Lorraine : LORIA, Technopôle de Nancy-Brabois - Campus scientifique
615, rue du Jardin Botanique - BP 101 - 54602 Villers-lès-Nancy Cedex (France)
Unité de recherche INRIA Rhône-Alpes : 655, avenue de l'Europe - 38330 Montbonnot-St-Martin (France)
Unité de recherche INRIA Rocquencourt : Domaine de Voluceau - Rocquencourt - BP 105 - 78153 Le Chesnay Cedex (France)
Unité de recherche INRIA Sophia Antipolis : 2004, route des Lucioles - BP 93 - 06902 Sophia Antipolis Cedex (France)

Éditeur
INRIA - Domaine de Voluceau - Rocquencourt, BP 105 - 78153 Le Chesnay Cedex (France)
http://www.inria.fr
ISSN 0249-6399